cobalt being plotted vs. the total metal concentration in the water at equilibrium. This gave the same trends as nickel. That the distribution coefficient of cobalt or nickel in a mixture of the two depends only on the total metal concentration is concluded.

Separation Factors

When cobalt and nickel were equilibrated separately with no nitric acid present, and the initial concentration was 100 g. each metal/liter, the calculated separation factor was a maximum at 1.49. When the two metals were equilibrated together, the actual separation factor was 1.27 for the same concentrations. Hence having both metals present decreased the maximum separation factor by about 15%. These separation factors in Table 3 are all low and constant at about 1.26. The separation factor for sulfates increased slightly when the metals were equilibrated together and was between 1.2 to 1.5 depending on the sulfuric acid concentration (*7*). The separation factor for the chlorides increased very greatly with increases in hydrochloric acid concentration (*3*).

Phase Diagram

The phase diagram (Figure 6) is shown for the ternary system *n*-butanol–nitric acid–water on a metal-free basis; it is very similar to the *n*-butanol–sulfuric acid–water system (*8*). When the metal salts cobalt or nickel nitrate are present, the solubilities of the alcohol in the aqueous phase and the aqueous phase in the alcohol phase are lowered and change the phase diagram markedly (Figure 6). Densities were determined and reported in Tables 2 and 3 and elsewhere (*6*).

Inspection of experimental phase solubility and tie line data, reported elsewhere (*1*) and used to plot Figure 6 show that the ratio of the nitric acid content to the water content in the phases at equilibrium are as follows. In the aqueous phase the ratio varies from 0.03 to 0.08 depending on the concentration of nitric acid. In the organic phase the ratio is about 0.2 to 0.8. Hence at equilibrium the nitric acid to water ratio is considerably higher in the organic than in the aqueous phase, and the acid is extracted preferentially by the organic solvent.

Using the triangular diagram (Figure 6) and Figures 1, 3, 4, or 5 one can predict the compositions and amounts of the two phases resulting fron the equilibrium of equal volumes of an aqueous solution and the solvent. Density data can then be used to calculate relative volumes of the resultant equilibrium solutions.

ACKNOWLEDGMENT

Grateful acknowledgement is made to the American Cyanamid Company for their fellowships which aided in this work.

NOTATION

C = concentration, g. metal/liter (not g. metal salt/liter)
C_0 = equilibrium concentration of metal or nitric acid in organic phase, g./liter
C_w = equilibrium concentration of metal or nitric acid in aqueous phase, g./liter
C_w' = concentration of metal or nitric acid in aqueous phase before extraction, g./liter
K = distribution coefficient, C_0/C_w
K' = distribution coefficient, $C_0/(C_w)^n$
n = constant

Greek Letters

β = separation factor = K(cobalt)/K(nickel)
ρ_0 = density of organic phase at equilibrium, g./ml.
ρ_w = density of aqueous phase at equilibrium, g./ml.

LITERATURE CITED

1. Geankoplis, C. J., and E. J. Scharf, *Doc.* 5827, A.D.J. Auxiliary Publications Project, Washington, D. C.; $1.25 for photoprints or 35-mm. microfilm.
2. Gagnon, J., *Chemist Analyst*, No. 1, **43**, 15 (1954).
3. Garwin, Leo, and A. N. Hixson, *Ind. Eng. Chem.*, **41**, 2298, 2303 (1949).
4. Moore, T. E., R. J. Laren, and P. C. Yates, *J. Phys. Chem.*, **59**, 90 (1955).
5. Rigamonti, R., and E. Spaccemela-Marchetti, *Chim. e ind. (Milan)*, **36**, 91 (1954).
6. Scharf, E. J., Ph.D. dissertation, Ohio State Univ., Columbus, Ohio (1957).
7. Schlea, C. S., and C. J. Geankoplis, *Ind. Eng. Chem.*, **49**, 1056 (1957).
8. Schlea, C. S., Ph.D. dissertation, Ohio State Univ., Columbus, Ohio (1955).
9. Snell, F. D., and C. T. Snell, "Colorimetric Methods of Analysis," 3 ed., Vol. II, p. 346, D. Van Nostrand, New York (1948).
10. Templeton, C. C., and L. K. Daly, *J. Am. Chem. Soc.*, **73**, 3989 (1951).
11. ———, *J. Phys. Chem.*, **56**, 215 (1952).
12. Yoe, J. H., "Photometric Chemical Analysis," Vol. I, p. 172, John Wiley, New York (1948).

Manuscript received September 5, 1957; revision received March 19, 1958; paper accepted March 20, 1958.

Heat and Mass Transfer from Wall to Fluid in Packed Beds

SAKAE YAGI and NORIAKI WAKAO

University of Tokyo, Tokyo, Japan

Experiments of heat and mass transfer from the tube wall to the fluids flowing through the packed beds were carried out separately. In heat transfer air was used as the fluid, and several kinds of solid particles with low and high thermal conductivities were investigated to determine effective thermal conductivities and wall heat transfer coefficients. In mass transfer the dissolution rate of the coated material on the inner wall of the packed tube to the water stream was measured, and wall mass transfer coefficients were analyzed. It was found that a close similarity exists between the J_H and J_D factor for the wall coefficients in the turbulent-flow region.

The rate of heat transfer in a packed bed is of particular interest in the process design not only of heat exchangers but also of catalytic reactors. The problem of the rate of heat transfer from the tube wall to a fluid flowing through a packed tube has been the subject of considerable study. The first work of heat transfer in a packed bed was made by Colburn (*6*) in 1931. He correlated the data as the over-all heat transfer coefficients, which are similar to those for an empty tube. Thereafter several investigators (*4, 12, 13*) reported the correlations for over-all coefficients.

For the calculation of the temperature distributions and explanation of the mechanism of heat transfer in the bed, the concept of the so-called "effective thermal conductivity" was introduced. Smith et. al. (*21*) determined values of the local effective thermal conductivity in the packed bed and found that the resistance to heat transfer increased greatly near the wall. Hatta and Maeda (*15*), Coberly and Marshall (*5*), and later workers (*2, 9, 18, 19, 23*) found that an additional resistance to heat transfer existed at the wall. They assumed the effective thermal conductivity to be constant within the bed and expressed the additive effect in the wall vicinity as the wall heat transfer coefficient.

This paper reports the results of both heat and mass transfer from the wall of

Table 1. Solid Particles Used For Heat Transfer Experiments.

G.S.—glass spheres
C.C.—cement clinkers (granular)
L.S.—lead shots (spherical)
S.B.—steel balls (spherical)

Reactor type 1
Diameter of tube: D_T = 36 mm., height: L = 200 mm.

Reactor type 2
D_T = 36 mm., L = 360 mm.

Run	Reactor type	Solid material	Particle size* (Tyler mesh range)	Average diameter of particle D_p, mm.	D_p/D_T
(A)	2	G.S.	20–24	0.764	0.0212
(B)	1	G.S.	20–24	0.764	0.0212
(C)	2	G.S.	16–20	0.909	0.0252
(D)	1	G.S.	16–20	0.909	0.0252
(E)	1	G.S.	—	2.60	0.0722
(F)	1	G.S.	—	6.00	0.167
(H)	2	C.C.	12–14	1.28	0.0355
(I)	2	C.C.	9–10	1.81	0.0503
(J)	1	C.C.	8–10	1.97	0.0547
(K)	2	C.C.	7–8	2.57	0.0714
(L)	1	C.C.	4–5	4.31	0.120
(N)	2	L.S.	20–24	0.764	0.0212
(O)	2	L.S.	14–16	1.08	0.0300
(P)	1	L.S.	—	1.50	0.0417
(Q)	1	S.B.	—	3.10	0.0861

*Geometrical mean size was taken as D_p.

Table 2. Comparison of Experimentally Observed Temperatures Along Center Axis of Bed With Calculated Temperatures

Run (F) − 1
Diameter of bed: D_T = 36 mm.
Height of bed: L = 200 mm.
Solid particles: glass spheres, D_p = 6.00 mm.
Air mass velocity: G = 2,740 kg./(sq. m.)(hr.)
Tube wall temperature: t_w = 100°C.
Inlet air temperature: t_0 = 16.5°C.

Bed height: l, cm.	Temperature at center axis of bed: t_c, °C. Observed values	Calculated values from Equation (2)
0	16.9	
4	21.9	19.9
8	35.3	33.5
12	49.3	47.8
16	61.1	59.4
20	69.8	68.5

Mixed mean temperature of effluent air: $(t_m)_L$,
observed value = 78.8°C.
calculated value from Equation (2) = 77.9°C.

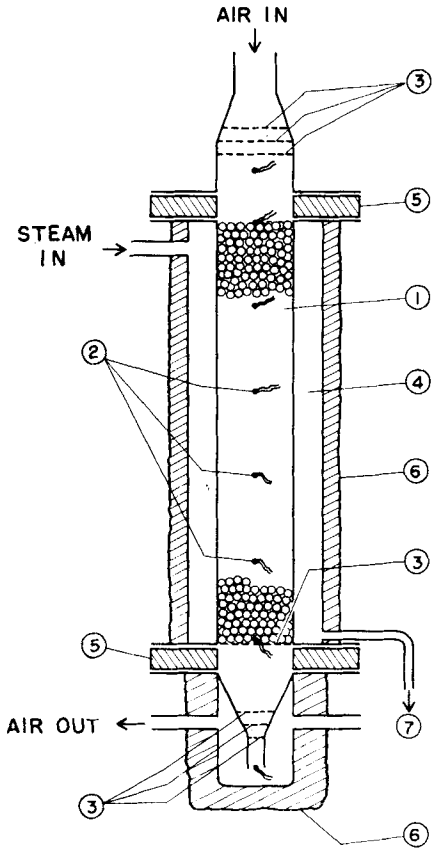

Fig. 1. Schematic diagram of reactor used for heat transfer experiment. (1) packed bed, (2) thermocouple, (3) screen, (4) steam jacket, (5) bakelite ring plate, (6) asbestos, (7) steam trap.

the packed tube to fluid flowing through the beds investigated separately. At first the effective thermal conductivities and wall heat transfer coefficients were determined for various kinds of solid particles in the heat transfer experiment. Then the wall mass transfer coefficients were obtained from the mass transfer experiment. The relationship between heat and mass transfer on the coefficient will be discussed.

HEAT TRANSFER EXPERIMENTS

Apparatus and Techniques

The main apparatus was a steam-jacketed, brass tube of 36-mm. I.D. with 1.0-mm. wall thickness. Two identical reactors with tubes of different lengths were used, the length of the shorter tube being 200 mm. and that of the longer one 360 mm. The experimental apparatus of the shorter tube is shown in Figure 1. The tube was packed with solid particles until their top level coincided with the upper steam-jacket flange. Thick Bakelite ring plates and rubber packing sheets were inserted between the flanges at either ends of the steam-jacketed tube to insulate heat from the heating section to the connecting ones. Steam was introduced at the top of the jacket, and the condensate was withdrawn through the trap.

Various temperature measurements were made by means of the copper-constantan thermocouple leads of 0.1-mm. diameter which were connected to a potentiometer. Prior to entering the packed bed the air passed successively through several sheets of screen, which obtained uniform flow and temperature distributions. The temperature of the inlet air was measured by the thermocouples located about 20 to 25 mm. above the entrance of the bed. The range of the inlet air temperature was from 10° to 30°C. The air stream was heated while flowing downward through the bed under the condition of uniform wall temperature. The longitudinal temperature gradients along the center axis of the tube were measured at every 40-mm. depth from the inlet to the exit of the bed. Mixing of the effluent air was done by passing it through three sheets of screen placed in the throttle of the adapter, which was made of the heat-insulating material to avoid heat loss. Just below the last screen a thermocouple was set to measure the mixed mean temperature of the effluent air; the preliminary runs assured that the correct mean temperature could be obtained this way.

The temperature difference between the saturation steam and outer surface of the tube was calculated by the equation for the film type of condensation (*16*) and found to be negligible for the purpose. The temperature drop through the wall of the brass tube was also negligible. The temperature of the inner surface of the packed tube was then taken as the temperature of the saturation steam in the jacket, 100°C. for all operating runs. After steady state was achieved, the necessary data were recorded.

The solid particles used in this investigation were glass spheres, broken solids of cement clinker, lead shots, and steel balls ranging from 0.764 to 6.00 mm., as tabulated in Table 1. For the solid particle cut by the Tyler sieves, the geometrical mean particle size was adopted; the square root of the product of the two adjacent sieve openings was taken as the mean particle diameter. The modified Reynolds number based on particle diameter varied from 20 to 800 in this experiment.

Calculations and Results

In a cylindrical packed tube heated from the wall the following partial differential equation for the temperature at steady state may be used:

$$C_p G \frac{\partial t}{\partial l} = k_e\left(\frac{\partial^2 t}{\partial r^2} + \frac{1}{r}\frac{\partial t}{\partial r}\right) \qquad (1)$$

TABLE 3. TYPICAL HEAT TRANSFER RESULTS

Run (refer to Table 1)	Air mass velocity G, kg./(sq. m.)(hr.)	Reynolds number D_pG/μ	Observed values: Inlet air temperature t_0, °C.	Observed values: Temperature at center of bed exit $(t_c)_L$, °C.	Observed values: Mixed mean temperature of effluent air $(t_m)_L$, °C.	* $-\frac{k_e\xi_1^2}{C_pG/2.303}$, cm.$^{-1}$	Derived results: k_e/k_g	Derived results: h_wD_p/k_g	Calculated temperatures from Equation (2), °C.: Temperature at center of bed exit	Calculated temperatures from Equation (2), °C.: Mixed mean temperature of effluent air
(F)-1	2,740	234	16.5	69.8	78.8	−0.0277	21.7	15.5	68.5	77.9
2	4,440	382	18.7	63.6	74.8	−0.0232	28.5	21.6	62.1	73.8
3	8,010	691	18.7	56.1	69.2	−0.0189	43.4	30.9	54.1	67.7
(I)-1	5,620	145	16.8	70.5	81.9	−0.0165	19.8	7.61	69.1	81.0
2	7,990	206	16.2	65.1	79.9	−0.0151	22.7	11.8	63.7	79.1
(K)-2	4,220	153	18.6	80.2	88.0	−0.0216	18.6	10.8	79.9	87.8
3	5,710	207	20.7	76.3	85.3	−0.0185	22.5	11.8	75.1	84.5
4	9,660	352	21.2	71.4	82.2	−0.0164	33.9	17.6	70.5	81.7
(O)-1	6,790	105	12.0	69.4	82.2	−0.0172	22.4	6.70	68.2	81.6
2	9,120	141	12.7	58.0	77.7	−0.0137	20.9	9.98	56.5	76.9

*Slope of straight-line portion in plot of $t_w - t_c$ vs. bed height on semilogarithm graph paper.

In the derivation of Equation (1) the following assumptions were made: (1) the temperature difference between solid and fluid is negligible; (2) the mass velocity of fluid is uniform across the tube diameter, and the physical properties of fluid are independent of temperature variation; (3) the effective thermal conductivity is uniform within the bed; and (4) the longitudinal heat conduction is negligible.

A solution of Equation (1), which may be easily obtained, has already been described by Hatta and Maeda (*15*) and Coberly and Marshall (*5*) using the following boundary conditions for the uniform inlet temperature and constant wall temperature:

at the inlet:
at $l = 0, \quad t = t_0$
at the inside surface of the tube wall:
at $r = R, \quad k_e(\partial t/\partial r) = h_w(t_w - t)$

The solution of Equation (1) with these boundary conditions is (*5, 15*)

$$\frac{t_w - t}{t_w - t_0} = 2\sum_{i=1}^{\infty} \frac{(h_wR/k_e)\cdot J_0(r\xi_i)\cdot e^{-k_e\xi_i^2 l/C_pG}}{[(h_wR/k_e)^2 + (R\xi_i)^2]\cdot J_0(R\xi_i)} \qquad (2)$$

The term ξ_i is a root of the following transcendental equation:

$$(h_wR/k_e)\cdot J_0(R\xi_i) = (R\xi_i)\cdot J_1(R\xi_i) \qquad (3)$$

For regions of sufficiently large values of l it is enough to take only the first term, $i - 1$, of the series in Equation (2). The effective thermal conductivity and the wall heat transfer coefficient are calculated simultaneously from the slope of the straight-line portion in the plot of $t_w = t_c$ against l on a semilogarithmic graph paper, the ratio of the temperature difference at the bed exit, $[t_w - (t_m)_L]/[t_w - (t_c)_L] = 2\cdot J_1(R\xi_1)/(R\xi_1)$, and with the aid of Equation (3).

Table 2, for a typical run, shows the observed temperatures along the center axis of the tube and those calculated with the help of Equation (2), which uses the derived results of k_e and h_w. It appears that the calculated temperatures are somewhat lower than the observed ones, owing to the inlet air being heated between the point of temperature measurement and the entrance to the bed, as pointed out by Coberly and Marshall (*5*).

The typical heat transfer results and the data from which they were derived are shown in Table 3.*

The temperature selected to evaluate the fluid properties is the arithmetical mean of the inlet and outlet temperatures.

The relation of k_e/k_g with $Re_p = D_pG/\mu$ is shown for glass spheres and broken solids of cement clinker in Figure 2 and for metal spheres in Figure 3. It seems permissible to express the values of the effective thermal conductivity by the following equation (*20, 22*) if some scattering of points at the relatively low Reynolds number is neglected:

$$k_e/k_g = k_e^0/k_g + (k_e)_{td}/k_g = k_e^0/k_g + (\alpha\beta)_H\cdot Pr\cdot Re_p \qquad (4)$$

where $(\alpha\beta)_H$ is the parameter for characterizing the fluid mixing in radial direction and is defined as the inverse of the modified Peclet number for heat transfer due to turbulent diffusion of fluid, $(Pe_H)_{td} = D_pC_pG/(k_e)_{td}$. The values of the terms in the right-hand side of Equation (4) may be determined for the experimental range employed in the present work as follows:

for glass spheres and broken solids of cement clinker

$$k_e^0/k_g = 6.0$$

$$(\alpha\beta)_H = 0.11 \quad \text{for} \quad D_p/D_T = 0.021 \sim 0.072$$

$$(\alpha\beta)_H = 0.09 \quad \text{for} \quad D_p/D_T = 0.12 \sim 0.17$$

for metal spheres

$$k_e^0/k_g = 13$$

$$(\alpha\beta)_H = 0.11 \quad \text{for} \quad D_p/D_T = 0.021 \sim 0.086 \qquad (5)$$

The values of $(\alpha\beta)_H$ in the present investigation agree well with the theoretical estimates on the basis of the "random walk" theory of Baron (*1*) and Ranz (*20*), and they also agree well with the experimental values of the previous investigators (*2, 5, 15, 18, 19, 22*). The value of k_e^0/k_g, which is the ratio of the effective thermal conductivity in stagnant

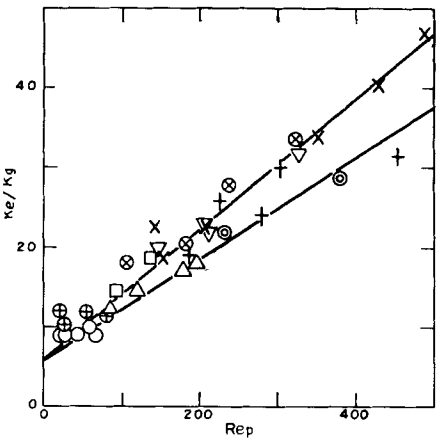

Fig. 2. Correlation of effective thermal conductivities for glass spheres and broken solids of cement clinker. (For symbols see Figure 4.)

*Tabular material has been deposited as document 5828 with the American Documentation Institute, Photoduplication Service, Library of Congress, Washington 25, D. C., and may be obtained for $2.50 for photoprints or $1.75 for 35-mm. microfilm.

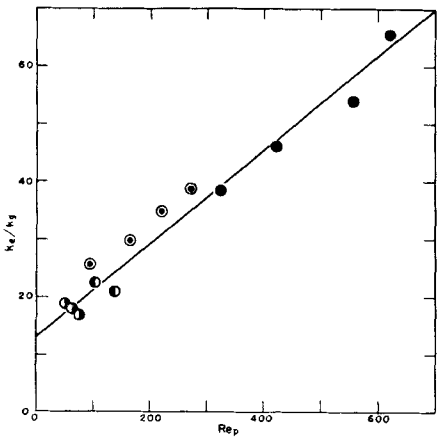

Fig. 3. Correlation of effective thermal conductivities for metal spheres. (For symbols see Figure 4.)

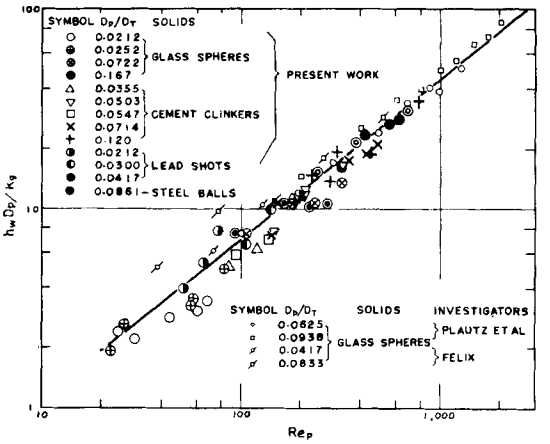

Fig. 4. Plot of wall heat transfer coefficients, for glass spheres, broken solids of cement clinker, and metal spheres of present work with data of Plautz and Johnstone (*18*), and Felix (*9*) for glass spheres. Where Felix's data were taken from the literature (*11*) and $\epsilon = 0.4$ was assumed.

fluid system to the molecular thermal conductivity of the fluid, for metal spheres was obtained as about twofold greater than that for glass spheres and cement clinker particles. The temperature level in the bed was less than 100°C. in all runs; the radiation contribution to k_e^0 may be neglected. The thermal conductivities of the glass and cement clinkers were less than 1 kcal./(m.)(hr.)(°C.), and those of lead and steel were about 30 and 40 kcal./(m.)(hr.)(°C.), respectively. Therefore it is apparent that the difference between the value of k_e^0 for glass spheres and cement clinker particles and that for metal spheres is due to the large difference of the thermal conductivities of the solid particles themselves. The values of k_e^0 agree with the theoretical estimates of Yagi and Kunii (*22*).

The data of the wall heat transfer coefficient were plotted as $h_w D_p/k_g$ against Re_p in Figure 4, and it was found that the wall coefficient was not so affected by the thermal conductivity of solid particles. The results of Plautz and Johnstone (*18*) for ½-, and ¾-in. glass spheres in an 8-in. tube, and those of Felix (*9*) for ⅛-, and ¼-in. glass spheres in a 3-in. tube were added in Figure 4; both of them are for the heating of air flowing in an upward direction through the packed beds. The results of the present investigation were not only for the spheres but also for the broken solids. All data of the present work were obtained by the heating of air flowing downward through the beds. Although the data of Felix, Plautz, et al. seem somewhat larger than those of the present work, the agreement of both sets of results is remarkable in view of the difference in experimental method. The solid line in Figure 4 can be represented by

$$h_w D_p/k_g = 0.18 Re_p^{0.80} \qquad (6)$$

The effect of the power of the Prandtl number in the correlation was not determined because the Prandtl number of air had a constant value of 0.70. According to the J factor of Chilton and Colburn (*3*), correlated by $J_H = (h_w/C_p G)(C_p\mu/k_g)^{2/3}$ for heat transfer, Equation (6) may be rewritten as

$$J_H = 0.20 Re_p^{-0.20} \qquad (6a)$$

The data for cylinders (*5*, *9*) are notably higher than those for spheres and broken solids owing to the difference in the contact manner of particles adjacent to the wall. Hanratty (*11*) showed that the wall heat transfer coefficient on cylinders varied with the fluid velocity to the 0.5 power, and he tried to interpret the mechanism of wall heat transfer by applying the *surface renewal* theory of Danckwerts (*8*).

MASS TRANSFER EXPERIMENTS

Apparatus and Techniques

To explore the relationship between the wall coefficients of heat and mass transfer the rate study of the dissolution of an organic solid coated on the inner wall of the packed tube to the water stream was carried out.

Two-naphthol was chosen for the diffusing solute because of relatively low solubility, known data of the diffusion coefficient, and easy measurement of concentration. The inner wall of the tube was coated by melting 2-naphthol of chemical-pure degree. The coated tube with a circular cross section and smooth inner surface was packed with solid particles.

The city water was introduced to the bed, and the flow was always downward to prevent fluidization of solid particles. When steady state was attained, the effluent water was sampled and analyzed by means of a spectrophotometer at the wave length of 2,850 Å.

Solubility and diffusion coefficient data on the system of 2-naphthol-water had been determined by Moyle and Tyner (*17*). Solubility of coated material checked experimentally, was found to agree with the values in the literature, used here, within the range of the experimental error.

The 2-naphthol was relatively insoluble in water, and so the tube diameter did not change appreciably during a test. The solid particles used for this work were silver sand and glass spheres. The ranges of the particles and the tube dimensions are shown

Table 4. Solid Particles Used for Mass Transfer Experiments

S.S.—silver sand (granular)
G.S.—glass spheres

Run	Solid material	Particle size* (Tyler mesh range)	Average diameter of particle D_p, mm.	Diameter of bed D_T, mm.	Height of bed L, mm.	D_p/D_T	L/D_T
(*A*)	S.S.	16–20	0.909	16.0	94	0.0568	5.88
(*B*)	S.S.	20–24	0.764	11.4	75	0.0670	6.58
(*C*)	S.S.	20–24	0.764	11.0	108	0.0695	9.82
(*D*)	S.S.	20–24	0.764	10.8	150	0.0708	13.9
(*E*)	S.S.	16–20	0.909	11.6	49	0.0784	4.22
(*F*)	S.S.	16–20	0.909	11.0	108	0.0826	9.82
(*G*)	S.S.	16–20	0.909	10.8	150	0.0842	13.9
(*H*)	S.S.	16–20	0.909	10.7	75	0.0850	7.01
(*K*)	G.S.	20–24	0.764	16.0	100	0.0477	6.25
(*L*)	G.S.	14–16	1.08	16.0	94	0.0675	5.88
(*M*)	G.S.	14–16	1.08	11.3	49	0.0956	4.34
(*N*)	G.S.	14–16	1.08	11.0	108	0.0982	9.82
(*O*)	G.S.	—	2.50	16.0	100	0.156	6.25

*Geometrical mean size was taken as D_p.

TABLE 5. TYPICAL MASS TRANSFER RESULTS

Run (refer to Table 4)	Water velocity u_0, m./hr.	Temperature of effluent water, °C.	Reynolds number D_pG/μ	Concentration of 2-naphthol: Concentration of effluent water (C_m) L, g.-mole/liter $\times 10^{-4}$	Concentration of 2-naphthol: Saturated concentration C_s, g.-mole/liter $\times 10^{-4}$	Schmidt number Sc	Derived results: Over-all mass transfer coefficient k_0D_p/D_v	Derived results: Wall mass transfer coefficient k_wD_p/D_v	Derived results: Wall mass transfer coefficient $J_D = (k_w/u_0)Sc^{2/3}$
(A) -1	5.60	18.0	1.34	4.07	40.6	1,100	6.55	7.21	0.523
3	18.2	17.0	4.23	2.35	39.0	1,150	12.9	13.7	0.309
5	46.3	17.0	10.8	1.50	39.0	1,150	21.0	21.7	0.191
8	227	16.7	52.6	0.826	38.5	1,170	56.4	57.3	0.104
12	824	17.4	194	0.595	39.6	1,130	139	141	0.0700
(O)- 2	14.9	17.7	9.73	1.61	40.1	1,110	17.7	17.9	0.179
5	52.0	17.8	34.0	0.992	40.3	1,110	37.5	37.8	0.108
7	190	16.7	121	0.571	38.5	1,170	84.6	84.9	0.0668
9	680	17.2	438	0.516	39.2	1,140	262	263	0.0577
12	1,900	17.0	1,220	0.404	39.0	1,150	580	580	0.0453

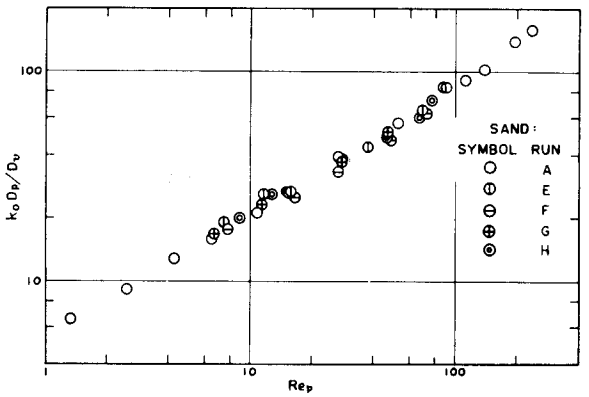

Fig. 5. Over-all mass transfer coefficients for 16 to 20 Tyler mesh of silver sand.

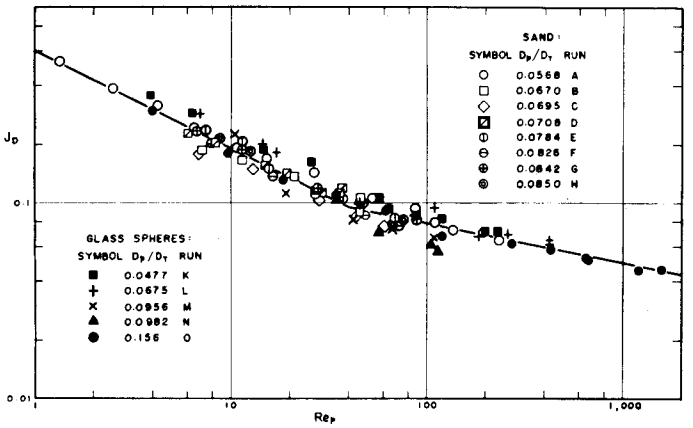

Fig. 6. Plot of J_D, based on wall mass transfer coefficient, vs. *Rep*.

in Table 4. In this experiment the modified Reynolds number was from 1 to 1,600, and the Schmidt number ranged from 1,000 to 1,700, depending on the temperature of water.

Calculations and Results

The following assumptions were made on the analysis of the mass transfer rate. The so-called "rodlike" flow occurs in the bed, and the concentration of solute in the fluid adjacent to the inner wall is saturated. Then for the mean concentration over the cross section the following differential equation is set up in the bed:

$$\pi D_T k_0(C_s - C_m)\, dl = (\pi/4)\, D_T{}^2 u_0\, dC_m$$

When one integrates and puts inlet concentration at zero,

$$k_0 = (D_T u_0/4l) \cdot \ln [C_s/(C_s - C_m)] \quad (7)$$

The derived results and the data from which they were computed are shown in Table 5 for typical runs.

The over-all mass transfer coefficients correlated to k_0D_p/D_v for 16 to 20 Tyler mesh of silver sand are plotted as a function of Re_p in Figure 5. An examination of the figure will show that values of the over-all mass transfer coefficients were not affected by the tube length and that the values of L/D_T were varied from 4.2 to 14. This was similar in experiments for other particles. It was made evident that the bed heights used in this experiment were long enough to obtain the converged values for over-all mass transfer coefficients which would be attained at the infinite bed length.

On the other hand, mass transfer from the wall to the flowing stream in the packed bed is analogous to the heat transfer phenomenon already described. At steady state the following partial differential equation for concentration of the diffusing solute may be written:

$$u_0 \frac{\partial C}{\partial l} = E\left(\frac{\partial^2 C}{\partial r^2} + \frac{1}{r}\frac{\partial C}{\partial r}\right) \quad (8)$$

The boundary conditions for this case are

at

$$l = 0, \qquad C = 0$$

at

$$r = R, \qquad E(\partial C/\partial r) = k_w(C_s - C)$$

where the effective diffusivity was assumed to be uniform within the bed. The wall mass transfer coefficient was defined in the boundary condition at the inner surface of the wall. The solution of Equation (8) is indicated directly for the mass transfer analogue from Equation (2) for the heat transfer. For the mean concentration the following equation is available:

$$\frac{C_s - C_m}{C_s} = 4 \sum_{i=1}^{\infty} \frac{e^{-E\xi_i{}^2 l/u_0}}{(R\xi_i)^2 \cdot [1 + (E\xi_i/k_w)^2]} \quad (9)$$

where ξ_i is defined by

$$k_w \cdot J_0(R\xi_i) = (E\xi_i) \cdot J_1(R\xi_i) \quad (10)$$

In a manner similar to the theoretical

development for heat transfer (*15*) the theoretical relation between k_w, E, and k_0 may be derived. The bed could be regarded as sufficiently long in this experiment. When one substitutes into Equation (7) the equation which is simplified by taking the first term in Equation (9) and putting $l = \infty$,

$$k_0 = E\, D_T \xi_1^2/4 \qquad (11)$$

results, where

$$k_w \cdot J_0(R\xi_1) = (E\xi_1) \cdot J_1(R\xi_1) \qquad (10a)$$

The effective diffusivity for mass transfer is the sum of the molecular diffusion and the diffusion process caused by turbulent mixing of fluid through the interstices of the bed. Usually the former contribution may be neglected as compared with the latter. Although there are several additional mechanisms that come into play for heat transfer which are not possible for mass transfer, for example transport of heat through the particles, the modified Peclet number for mass transfer $Pe_D = D_p u_0/E$ was assumed to be equivalent to the value of $(Pe_H)_{td} = D_p C_p G/(k_e)_{td}$ for heat transfer.

$$E/D_v = (\alpha\beta)_D \cdot Sc \cdot Re_p \qquad (12)$$

where $(\alpha\beta)_D$ was assumed to be 0.11. Using Equations (10*a*), (11), and (12) one can obtain the values of the wall mass transfer coefficient from data of the over-all mass transfer coefficient.

The calculated results of k_w were listed in terms of $k_w D_p/D_v$ and $J_D = (k_w/u_0)(\mu/\rho D_v)^{2/3}$ in Table 5.* It should be noted that values of k_w are larger than those of k_0 by less than 10%, because of a little contribution of the eddy diffusivity on the over-all dissolution rate for the sake of the large values of the Schmidt number in this system. Plautz and Johnstone (*18*) reported that the value of $(\alpha\beta)_D$ was about 25% below that of $(\alpha\beta)_H$. Even if their result is used for the present calculation, it has little effect on the calculated results of the wall coefficient. The calculated data of the wall mass transfer coefficient are plotted to J_D against Re_p in Figure 6. The data of the glass spheres and those of silver sand agreed well with the solid lines represented by the equations

$$J_D = 0.60 Re_p^{-\frac{1}{2}}$$

for laminar flow,

$$Re_p = 1 \sim 40 \qquad (13)$$

$$J_D = 0.20 Re_p^{-0.20}$$

for turbulent flow,

$$Re_p = 40 \sim 2{,}000 \qquad (14)$$

*Tabular material has been deposited as document 5828 with the American Documentation Institute, Photoduplication Service, Library of Congress, Washington 25, D. C., and may be obtained for $2.50 for photoprints or $1.75 for 35-mm. microfilm.

It has been generally recognized that the flow through the packed bed became turbulent at Re_p exceeding about 40, and this appeared in the correlations for the wall mass transfer coefficient as expressed by Equations (13) and (14).

DISCUSSION ON WALL COEFFICIENT

The Prandtl number was omitted in Equation (6) for the wall heat transfer coefficient because it remained constant, 0.70, for air. In the mass transfer experiment the Schmidt number of the 2-napththol-water system was limited in the range of 1,000 to 1,700; therefore the effect of the Schmidt number on the wall mass transfer was not determined. But from comparison of Equation (6*a*) with Equation (14), it is interesting to note that the same equations of the Reynolds number were obtained for wall coefficients on heat and mass transfer, as far as the data were correlated to the J factor (Figure 7). The present investigation for heat transfer was carried out in the turbulent flow region only, because at the low flow rate it was difficult to obtain exact data owing to the small driving force at the outlet of the bed. On the contrary the experiment of mass transfer could be easily extended to the low Reynolds-number region. The mechanism of heat transfer at the inside of the tube wall is more complicated than that of mass transfer, since heat is transferred through the solid particles adjacent to the wall in addition to being transferred by the fluid flow. Even if the wall heat transfer coefficient is affected by the former contribution, it will be little in comparison with the latter in the turbulent-flow region, because the analogy of the J factor was confirmed to exist between heat and mass transfer.

On the study of the transfer rate from particle to fluid in the packed bed Ranz (*20*) proposed the model theory that the particle in the bed could be ragarded as a single particle obtaining an actual velocity of jet flowing through a minimum open area formed by particles. For the rhombohedral packing of spheres the ratio of the total cross section to the open area effective for jet formation was calculated as 10.7, and for the data of Gamson, Thodos, and Hougen (*10*) on the transfer rate from particle to fluid in the packed bed the effective fluid velocity was obtained as 9.1 times the superficial one.

The dependence of the wall mass transfer coefficients on fluid velocity were similar to that for flow over the flat plate in both of the laminar- and turbulent-flow regions. The interpretation of experimental equations for wall coefficients in the turbulent-flow region was attempted by use of the discontinuous boundary-layer model, which means that the boundary layer at the wall is continually replaced with fresh fluid caused by turbulent mixing. In this model theory the wall is assumed to be covered with discontinuous boundary layers having the same length, and the resistance to heat transfer at the inner wall is assumed to be due to the boundary layer existing there. For the interpretation of heat transfer in the fluidized bed a similar model was applied by Levenspiel and Walton (*14*).

The equation of the wall coefficient in the turbulent flow was obtained by proposing the following simplified models: (1) The effective fluid velocity, nine times the superficial one, makes the discontinuous boundary layers on the wall. (2) The average length of each boundary layer is equal to the diameter of solid particle; the boundary layer develops from the contact point of solid particle adjacent to the wall, is destroyed at the next contact point on the wall, and is replaced with fresh boundary layer. (3) The rate of heat and mass transfer in the boundary layer is similar to that of a flat plate. For the mean heat transfer coefficient in the turbulent flow of a fluid parallel to a flat plate the Colburn relation (*7, 16*) has been suggested:

$$h_w x/k_g = 0.036 Pr^{\frac{1}{3}} (xv\rho/\mu)^{0.8}$$

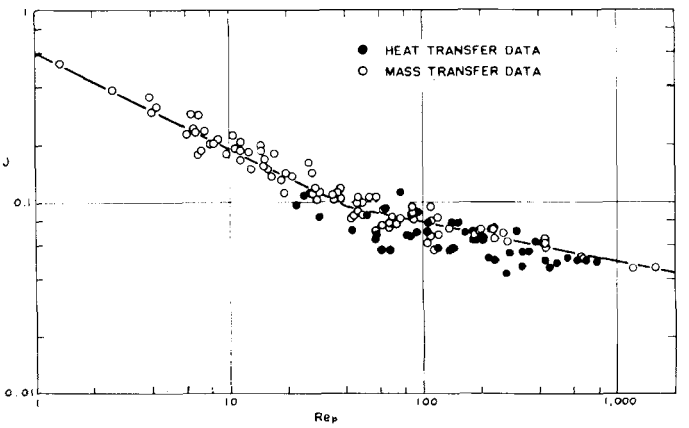

Fig. 7. Comparison of J_H and J_D for wall coefficient of present work.

Substituting $9u_0$ for v and D_p for x, one has

$$J_H = 0.21(D_p u_0 \rho/\mu)^{-0.2} \quad (15)$$

The same equation will be derived for J_D of mass transfer. Equation (15) agrees fairly well with the empirical correlations expressed by Equation (6*a*) for heat transfer and by Equation (14) for mass transfer.

CONCLUSIONS

Heat and mass transfer from the tube wall to the fluid flowing through the packed beds of various kinds of solid particles were investigated. Air was used as the fluid for heat transfer and water for mass transfer. The results obtained from the investigation were summarized as follows:

1. The effective thermal conductivity of the packed bed was found to be expressed by

$$k_e/k_g = 6.0 + 0.11 PrRe_p$$

for

$$D_p/D_T = 0.021 \sim 0.072$$

$$k_e/k_g = 6.0 + 0.09 PrRe_p$$

for

$$D_p/D_T = 0.12 \sim 0.17$$

for glass spheres and broken solids of cement clinker, and by

$$k_e/k_g = 13 + 0.11 PrRe_p$$

for

$$D_p/D_T = 0.021 \sim 0.086$$

for metal spheres.

2. The following correlation was obtained for the wall heat transfer coefficient:

$$J_H = (h_w/C_p G)Pr^{\frac{2}{3}} = 0.20 Re_p^{-0.20}, \qquad Re_p > 20$$

3. The following correlations for the wall mass transfer coefficient were obtained for silver sand and glass spheres:

$$J_D = (k_w/u_0)Sc^{\frac{2}{3}} = 0.60 Re_p^{-\frac{1}{2}}, \qquad Re_p < 40$$

$$J_D = (k_w/u_0)Sc^{\frac{2}{3}} = 0.20 Re_p^{-0.20}, \qquad Re_p > 40$$

NOTATION

C = concentration of solute in fluid, M/L^3
C_m = mixed mean concentration of solute in fluid over cross section, M/L^3
C_p = specific heat of fluid, Q/MT
C_s = saturated concentration of solute, M/L^3
D_p = diameter of packing particle, L
D_T = tube diameter, L
D_v = molecular diffusion coefficient, L^2/θ
E = effective diffusivity in radial direction, based on void plus nonvoid area, L^2/θ
G = superficial mass velocity of fluid based on empty tube, $M/L^2\theta$
h_w = wall heat transfer coefficient, $Q/L^2\theta T$
J_D = J factor correlating wall mass transfer coefficient = $(k_w/u_0)Sc^{2/3}$, dimensionless
J_H = J factor correlating wall heat transfer coefficient = $(h_w/C_p G)Pr^{2/3}$, dimensionless
$J_0( )$ = Bessel function of first kind of zero order, dimensionless
$J_1( )$ = Bessel function of first kind of first order, dimensionless
k_e = effective thermal conductivity in radial direction, based on void plus nonvoid area, $Q/L\theta T$
k_g = molecular thermal conductivity of fluid, $Q/L\theta T$
k_0 = over-all mass transfer coefficient, L/θ
k_w = wall mass transfer coefficient, L/θ
l = longitudinal distance variable, L
L = length of packed bed, L
Pe_D = modified Peclet number for mass transfer = $D_p u_0/E$, dimensionless
Pe_H = modified Peclet number for heat transfer = $D_p C_p G/k_e$, dimensionless
Pr = Prandtl number = $C_p\mu/k_g$, dimensionless
r = radial distance variable, L
R = radius of tube = $D_T/2$, L
Re_p = modified Reynolds number based on particle diameter = $D_p G/\mu$, dimensionless
Sc = Schmidt number = $\mu/\rho D_v$, dimensionless
t = temperature in packed bed, T
t_c = temperature at center axis of tube, T
t_m = mixed mean temperature of fluid over cross section, T
t_0 = inlet temperature of fluid, T
t_w = temperature of wall, T
u_0 = superficial fluid velocity based on empty tube, L/θ
v = velocity of main stream outside boundary layer, L/θ
x = length of boundary layer, L

Greek Letters

$(\alpha\beta)_D$ = $E/D_p u_0$, dimensionless
$(\alpha\beta)_H$ = $(k_e)_{td}/D_p C_p G$, dimensionless
ϵ = fractional void in bed, dimensionless
μ = viscosity of fluid, $M/L\theta$
ρ = density of fluid, M/L^3

Subscripts

L = bed exit
td = turbulent diffusion

Dimensions

L = length
M = mass
Q = quantity of heat
T = temperature
θ = time

LITERATURE CITED

1. Baron, Thomas, *Chem. Eng. Progr.*, **48**, 118 (1952).
2. Campbell, J. M., and R. L. Huntington, *Petroleum Refiner*, No. 2, **31**, 123 (1952).
3. Chilton, T. H., and A. P. Colburn, *Ind. Eng. Chem.*, **26**, 1183 (1934).
4. Chu, Y. C., and J. A. Storrow, *Chem. Eng. Sci.*, **1**, 230 (1952).
5. Coberly, C. A., and W. R. Marshall, Jr., *Chem. Eng. Progr.*, **47**, 141 (1951).
6. Colburn, A. P., *Ind. Eng. Chem.*, **23**, 910 (1931).
7. Colburn, A. P., *Trans. Am. Inst. Chem. Engrs.*, **29**, 174 (1933).
8. Danckwerts, P. V., *Ind. Eng. Chem.*, **43**, 1460 (1951).
9. Felix, J. R., Ph.D. thesis, Univ. Wisconsin, Madison (June, 1951).
10. Gamson, B. W., George Thodos, and O. A. Hougen, *Trans. Am. Inst. Chem. Engrs.*, **39**, 1 (1943).
11. Hanratty, T. J., *Chem. Eng. Sci.*, **3**, 209 (1954).
12. Kuzuoka, Tsuneo, *Chem. Eng. (Japan)*, **8**, 85 (1944).
13. (*a*) Leva, Max, *Ind. Eng. Chem.*, **39**, 857 (1947); (*b*) ———, and Milton Grummer, *ibid.*, **40**, 415 (1948); (*c*) Leva, Max, Murray Weintraub, Milton Grummer, and E. L. Clark, *ibid.*, p. 747; (*d*) Leva, Max, *ibid.*, **42**, 2498 (1950).
14. Levenspiel, Octave, and J. S. Walton, *Chem. Eng. Progr. Symposium Ser.* No. 9, **50**, 1 (1954).
15. (*a*) Hatta, Shiroji, and Shiro Maeda, *Chem. Eng. (Japan)*, **12**, 56 (1948), **13**, 79 (1949); (*b*) Maeda, Shiro, and Kenjiro Kawazoe, *ibid.*, **17**, 276 (1953), **18**, 279 (1954).
16. McAdams, W. H., "Heat Transmission," 3 ed., McGraw-Hill Book Company, Inc., New York (1954).
17. Moyle, M. P., and Mack Tyner, *Ind. Eng. Chem.*, **45**, 1794 (1953).
18. Plautz, D. A., and H. F. Johnstone, *A.I.Ch.E. Journal*, **1**, 193 (1955).
19. Quinton, J. H., and J. A. Storrow, *Chem. Eng. Sci.*, **5**, 245 (1956).
20. Ranz, W. E., *Chem. Eng. Progr.*, **48**, 247 (1952).
21. (*a*) Bunnell, D. G., H. B. Irvin, R. W. Olson, and J. M. Smith, *Ind. Eng. Chem.*, **41**, 1977 (1949); (*b*) Hall, R. E., and J. M. Smith, *Chem. Eng. Progr.*, **45**, 459 (1949); (*c*) Schuler, R. W., V. P. Stallings, and J. M. Smith, *Chem. Eng. Progr. Symposium Ser. No.* 4, **48**, 19 (1952); (*d*) Kwong, S. S., and J. M. Smith, *Ind. Eng. Chem.*, **49**, 894 (1957).
22. Yagi, Sakae, and Daizo Kunii, *Chem. Eng. (Japan)*, **18**, 576 (1954); *A.I.Ch.E. Journal*, **3**, 373 (1957).
23. Yagi, Sakae, Daizo Kunii, and Yasuto Shimomura, *Chem. Eng. (Japan)*, **21**, 342 (1957).

Manuscript received December 11, 1957; revision received March 17, 1958; paper accepted March 18, 1958.